Tropical Upper-Tropospheric Extended Clouds: Inferences from Winter MONEX

PETER J. WEBSTER AND GRAEME L. STEPHENS

CSIRO Division of Atmospheric Physics, Aspendale, Victoria, Australia.

(Manuscript received 5 March 1979, in final form 7 April 1980)

ABSTRACT

The most common cloud species observed during the Winter Monsoon Experiment (WMONEX) was thick (optically black) middle and upper tropospheric extended cloud. Data from the Geostationary Meteorological Satellite (GMS) showed the extended cloud to occupy half the near-equatorial South China Sea and Indonesia on some days with tops in the vicinity of the 200 mb level. Detailed observations from the WMONEX composite observing array indicated that the clouds extended up to 750 km from the convective source regions, possessed bases in the vicinity of the freezing level and lay above a generally suppressed and subsident lower troposphere. The observation of widespread precipitation from the extended cloud and the encountering of ice particles during the cloud penetrations suggest that the extended clouds are active in a diabatic heating sense.

Calculations using a radiative transfer model and cloud and atmospheric states derived from WMONEX data indicate substantial net heating at the base of the cloud ($\sim$20 K day^{-1}) and cooling at the top (-5 to -15 K day^{-1}), resulting in a heating rate differential between the base and top of the cloud of up to 35 K day^{-1}. Net heating or cooling occurs depending upon the diurnal cycle. It is conjectured that the effect of the radiative heating is to destabilize the cloud layer. As the magnitude of the radiative *heating* at the base of the cloud is at least within a factor of 2 of estimates of the *cooling* at the cloud base due to melting for moderate disturbances and relatively greater for weak disturbances or in locations well removed from the convective source in any disturbance, it is argued that radiative effects cannot be ignored in the calculation of the total diabatic heating fields in tropical cloud systems.

1. Introduction

The realization that there exist unique phenomena in the low latitudes and that such phenomena exert a profound influence on processes at higher latitudes has substantially increased interest in the meteorology of the tropical regions during the last two decades. During this period, a number of key problems associated with basic modeling have received considerable emphasis. The most notable is the consideration of convective processes and the general problem of scale interaction between subgrid-scale processes and those of larger scale. So important are the convective transports in the tropics that most effort appears to have focussed on their parameterization. In most parameterizations the cloud, or cluster of clouds, is treated as a one-dimensional entity and the transports related to the larger scale (prognostic) fields. The parameterizations consider diabatic processes but lend emphasis to latent heat release usually at the expense of other heating fields such as radiation. Further, the residual effects of the cloud clusters (middle and upper tropospheric extended clouds[1]) are generally ignored, even though the area they cover is perhaps an order of magnitude larger than the convective region itself. Possibly the principal reason for this neglect has been that such cloud decks have been assumed passive from a diabatic heating viewpoint.

Contrary evidence has emerged from the GARP Atlantic Tropical Experiment (GATE) and even earlier from the Line Islands Experiment. Extended middle and upper level cloud decks were found to be *strongly active* as both a radiative and latent heating source. For example, Albretcht and Cox (1975) and Cox and Griffith (1979) showed explicitly that upper level extended clouds interact strongly with and are instrumental in determining the local radiative field. That strong variations in radiative heating occur in both longitude and latitude was discussed in the theoretical study of Stephens and Webster (1979). They also showed that middle and upper cloud substantially influenced the character of the net radiative flux divergence in a manner which keenly depended on the cloud type and

[1] We use here the term middle and upper level extended cloud to avoid confusion with the proper term "stratus" or the more restrictive term "anvil." The former has come to refer commonly to low-level cloud whereas the latter refers to the outgrowth of convection in the vicinity of the convective source. As we will refer later to middle and upper level cloud removed hundreds of kilometers from the source region, we choose a more general term.

0022-4928/80/071521-21$09.25
© 1980 American Meteorological Society

height, as well as the latitude of the cloud deck. The potential for strong radiative-convective-dynamic coupling was hinted at by Stephens and Wilson (1980) who illustrated distinct sensitivity of convective parameterizations to the radiative heating profiles chosen. In summary, a large number of studies point toward substantial variations in both the magnitude and scale of the radiative heating function. Rather than the weak and fairly constant heating profile suggested by Dopplick (1972), the picture which has emerged is of a strong function varying rapidly in space with magnitudes in disturbed regions which are similar to the heating rates traditionally ascribed to latent heating functions. Radiative properties which refer particularly to extended clouds in the WMONEX region will be discussed in Section 4.

If the radiative arguments are sound, observations made during the Winter Monsoon Experiment (WMONEX) would suggest an important role for upper and middle tropospheric extended clouds in determining the radiative budget of the equatorial region. For long periods of December 1978 (Phase 1 of WMONEX) in the South China Sea–Indonesian region thick (optically black) altostratus and cirrostratus appeared as the predominant cloud species and extended hundreds of kilometers from convective source regions. Sources of the extended cloud could usually be traced to either synoptic-scale disturbances or to the considerable diurnal activity associated with the large islands of Indonesia. Regions of precipitation from the extended cloud decks were commonly observed.

Earlier field experiments in the western Pacific found considerable variability in the structure of disturbances and associated cloud fields (Malkus and Riehl, 1964). Of particular interest were the vast regions of upper level extended cloud, areas of which were observed to precipitate. Whereas it was generally assumed such cloud originated from convective debris, the observation of precipitation in the generally subsident and divergent "exterior" portion of the disturbance was surprising. Acknowledging this observation, the "Tropical Whole Sky Code" was developed to allow a detailed cataloging of the tropical atmosphere and substantial precipitation from the ". . . upper sheet . . ." is taken into account in classifications 13–16 (Malkus and Riehl, 1964) as typical of the disturbed tropical atmosphere.

Beyond the Malkus and Riehl study and the occasional reference in early observational, operationally oriented reports or manuals, the existence of stratiform precipitation in the tropics received scant attention in the literature. With the Line Islands Experiment and GATE a number of pertinent studies emerged. Most notable are those of Zipser (1977) and Houze (1977) who noted considerable anvil precipitation in propagating squall lines. Houze estimated that 40% of the total precipitation of the disturbance emanated from the anvil. Later work (Leary and Houze, 1979) suggested a complicated substructure of heating and cooling in the vertical relating to hydrometeor phase changes within the anvil. They suggested that substantial cooling due to *melting* at the base of the anvil accounted for cooling rates of the order of 1–7 K h^{-1} and cooling due to evaporation of water droplets *below* the anvil to be of the order of 0.2–6 K h^{-1} which cumulatively resulted in subsidence in the lower troposphere. As there was precipitation, a net heating was assumed in the main body of the anvil resulting in mean ascent. Horizontal inflow from the convective source near the melting layer satisfied the mass continuity constraints. *In all studies, including a numerical simulation by Brown (1979), radiative effects are not considered or are ignored.*

As the GATE studies of Zipser (1977), Leary and Houze (1979), and Houze (1977) are perhaps the best-documented tropical disturbance case studies, they will serve as useful base references for the present investigation. As such it is important to question whether or not the GATE disturbances are comparable with the WMONEX disturbances. Some differences in space and time scales seem apparent. The GATE squall lines were propagating phenomena with lifetimes of hours and horizontal scales [defined by the radar determined precipitation zone (Leary and Houze, 1979)] were between 100 and 200 km. In comparison, the WMONEX disturbances appeared to possess lifetimes of days and to possess horizontal scales (defined by the extent of the cloud canopy from satellite observation) in excess of 600 km from the convective centers. The systems are similar in that they possessed convective source regions and extensive middle and upper cloud systems which resembled nimbostratus. Detailed comparisons between the disturbances of the two regions must really await the analysis of the WMONEX radar data as it is radar which has formed the basics of the GATE analyses.

In summary, a number of questions arise:

1) What is the source of the extended middle and upper level cloud? Are the decks merely upper tropospheric debris from cloud clusters or are the middle-level extended cloud systems developed independently of the cumulonimbus cloud?

2) What are the maintenance mechanisms of the extended cloud systems at distances well away from the convective source regions? Are the space and time (longevity) scales determined merely by the amount of cloud debris pumped into the middle and upper levels or are other processes involved in perpetuating and maintaining the extended cloud decks?

3) What is the distribution of total diabatic heat-

ing associated with the cloud decks away from the convective sources and what is its influence on the state of the tropical atmosphere? Is the concept of strong radiative effects in the outflow region of convective systems compatible with the latent heating fields described by other workers?

The study has one further purpose. In the theoretical study of Stephens and Webster (1979), the potential climatic importance of extended cloud decks was discussed. The present paper may be thought of as one part of an ongoing study into the role of clouds in structures where dynamic and diabatic time scales are similar. Both climatic and low-latitude structures fall within this range.

In the following paragraphs, the WMONEX period will be referred to extensively. Whereas there are significant weaknesses in the data set for a study aimed at elucidating dynamic-cloud interactions, it does stand at the present time as a unique low-latitude ensemble. Even so, it would be foolish to suppose that the set is indicative of all low latitude regions; the South Asian-Indonesian region is unique from a meteorological viewpoint. Consequently, the paper should be considered as a discussion of tentative results and inferences from a pilot study aimed at establishing connections (if any) between the theory of Stephens and Webster (1979) and the reality of observed processes. Generalizations must await the establishment of a grander scheme; probably the completion of a cloud climatology based on remote sensing.

In the next section spatial scales of the upper level cloud will be identified as they existed during the entire period of WMONEX.

2. Cloud scales

From a radiative viewpoint, the depth, height and horizontal extent of the various cloud species are extremely important. Such information is critical in order to determine the three-dimensional distribution of the radiative state of the atmosphere and, consequently, the structure of the diabatic heating. In this section we will use the GMS (the Japanese Geostationary Meteorological Satellite which operates over 0°N, 140°E)[2] to establish the horizontal extent, the height of the cloud and to some extent its time scale. The data period corresponds to Phase 1 of WMONEX (i.e., December 1978).

The five-day mean cloud distributions for the area 90°E–170°W and 20°N–20°S are shown on Figs. 1a–1c. The upper panel of each diagram shows the *total* cloud in tenths and the lower panel the *upper* cloud. High cloud is defined as clouds which are cooler than the climatological ambient 400 mb temperature as sensed by the GMS. Regions of total cloud > 60% are stippled as are the upper level region where coverage exceeds 40%.

The total cloud fields show four major regimes. There are the equatorial maxima, the Northern Hemisphere maxima near 20°N and the two subtropical minima. The equatorial maximum extends across the domain and shows a bifurcation in the Central Pacific; the southern fork being associated with the South Pacific cloud band (Streten, 1973; Webster and Curtin, 1974). The bifurcation is also evident in the upper cloud amounts, most of which appear to be restricted to the equatorial region. In general, in the low latitudes total and upper level clouds possess strong positive correlation.

In the region of the WMONEX, the cloudiness distributions may be divided into two main categories. The first category occurs with the maximum cloudiness (total and upper) being concentrated in the near-equatorial Southern Hemisphere. Such periods were the 2–6 December, 22–26 December and 27–31 December 1978. Periods 12–16 and 17–21 December showed cloud maxima in the near equatorial Northern Hemisphere. The period 7–11 December possessed maxima in both hemispheres. Certain areas maintained maximum concentration of upper level clouds for successive 5-day periods. For example, the Java Sea region maintained upper level cloud coverage through three 5-day mean periods (e.g., 2–16 December) at > 60%. Similar persistence was observed along the near equatorial trough, especially in the region of the Southern Hemisphere Central Pacific cloud band and also northwest of Borneo in the South China Sea region during most periods.

Fig. 2 provides an indication of the cloud-top height of the distributions shown in the previous diagram (data obtained from JMSMR). Isopleths of the corresponding cloud top pressures are drawn for the three periods 2–06, 12–16 and 17–21 December 1979. Two major domains are apparent. In the equatorial regions, cloud top pressures are generally less than 200 mb, whereas further away from the equator cloud distributions rarely appear to penetrate the 700 mb level.

In summary, satellite data indicate that in the region of GMS coverage, middle-level extended cloud was a common and abundant species. Persistence of large coverage of the cloud in certain regions suggests that the cloud species are long-lived or are associated with persistent low latitude processes or phenomena. However despite some indications of the properties of low-latitude cloud cover the satellite observing platform cannot provide the *base level* of the extended clouds. All that is known is their geographic distribution and cloud-top height and that the clouds were optically black.

[2] In particular, data from the Monthly Report of the Meteorological Satellite Center, Tokyo, Japan, obtainable from Japanese Meteorology Service, Tokyo, Japan (referred to as JMSMR).

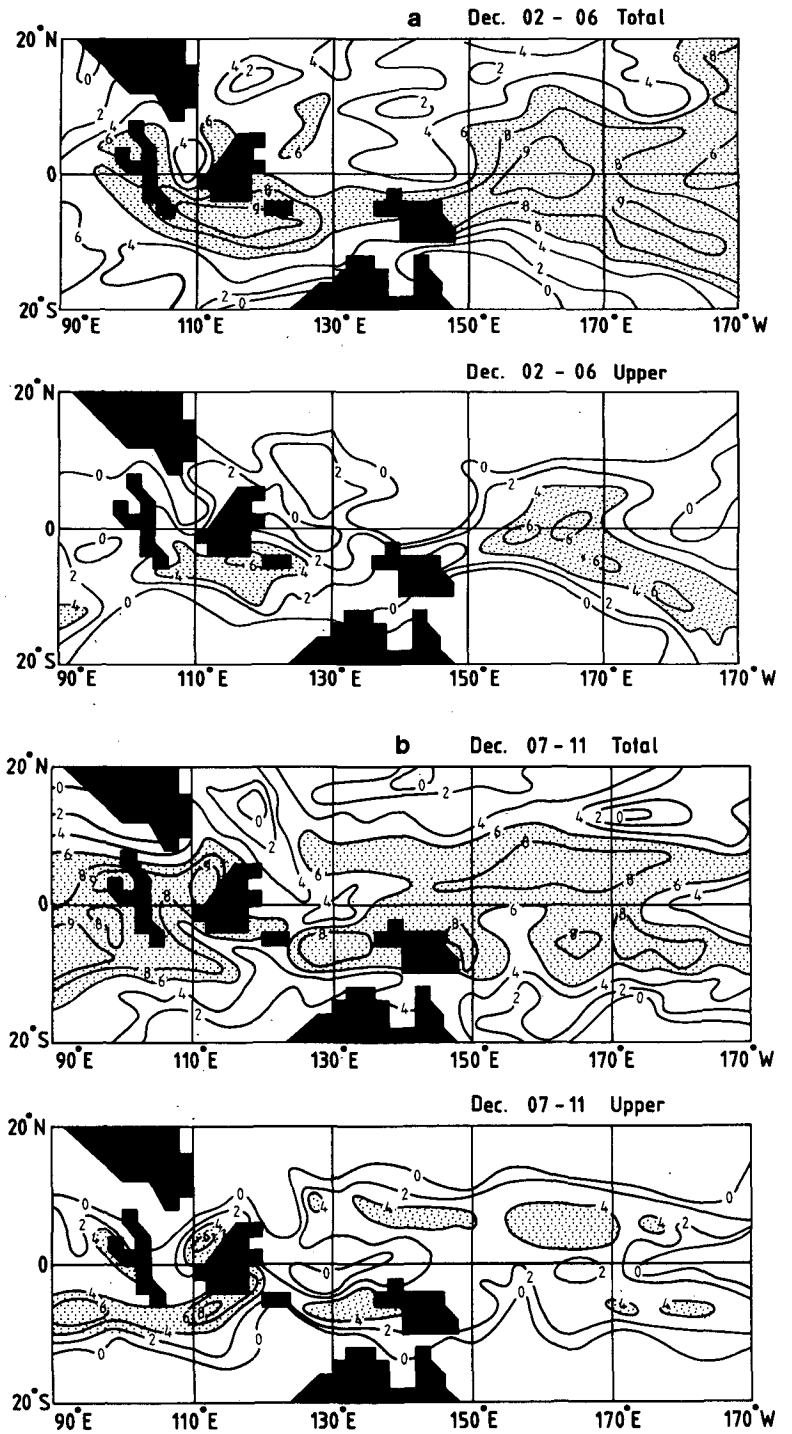

FIG. 1. Five-day average cloudiness distributions for total (upper panel) and upper (lower panel) cloud. Shaded areas denote > 0.6 total cloudiness or 0.4 upper cloudiness. Periods are (a) 2–6 December (b) 7–11 December (c) 12–16 December (d) 17–21 December (e) 22–26 December and (f) 27–31 December 1978 (units: tenths of cloud).

3. Observations

a. The WMONEX composite observing network

The composite observing array for Phase 1 of WMONEX (i.e., December 1978) contained five major components. These were an enhanced observing conventional network (both rawin and pibal), a number of special rawinradiosonde stations, a digitalized weather radar system, three research ships, and three dedicated research air-

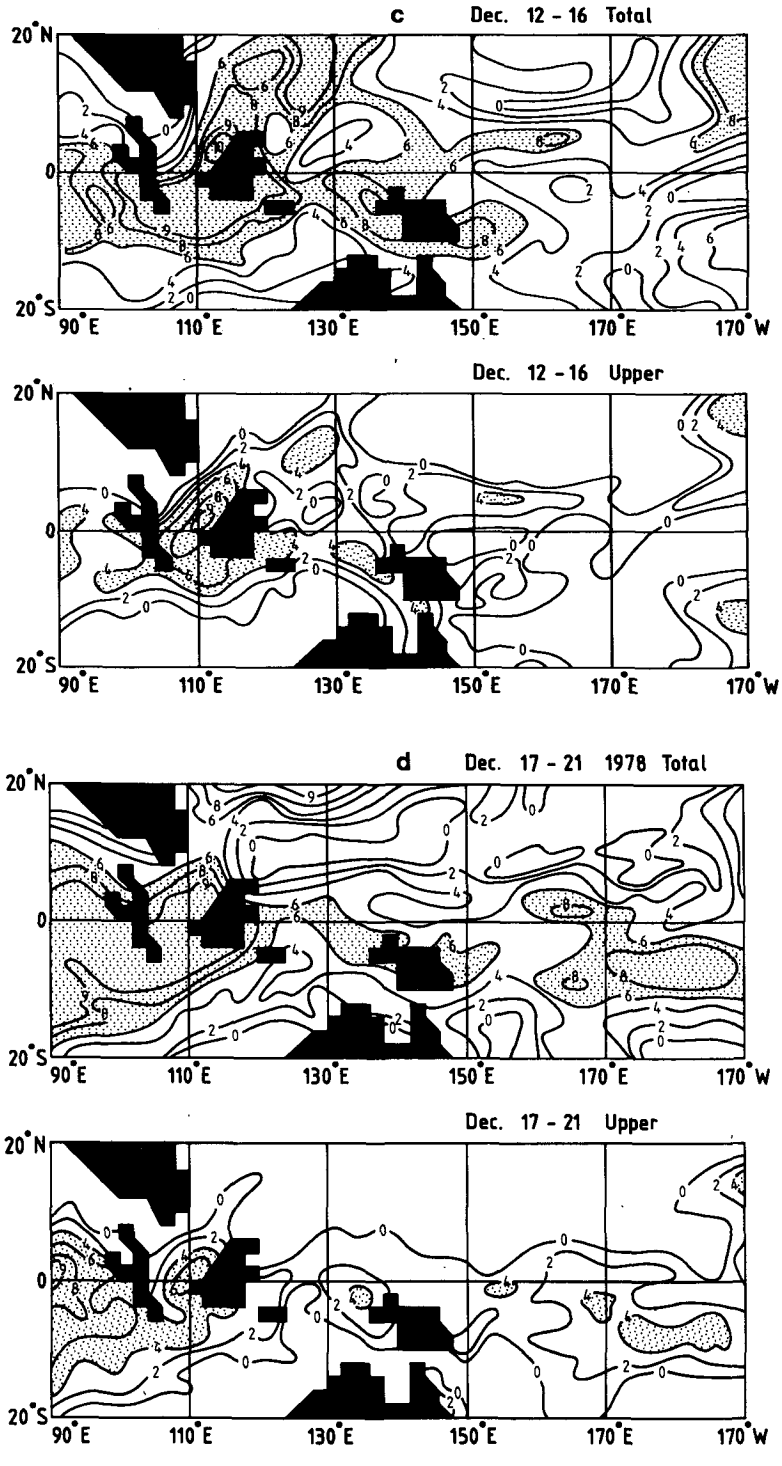

FIG. 1. (*Continued*)

craft. Of particular pertinence to this study are the two aircraft[3] which operated in the South China Sea out of Kuala Lumpur, Malaysia; the USA NOAA P-3 and the USA NCAR Electra, and the three USSR research ships located at 4°N, 111°E, 7°N, 111°E and 7°N, 109°E. Whenever possible, the two aircraft operated in the vicinity of the digital weather radar located at Bintulu, Sarawak. In addition, the GMS provided a periodic coverage of infrared and visible radiation fields as well as providing derived cloud vector winds.

[3] A third low-level aircraft provided by the Royal Hong Kong Observatory operated in the vicinity of Hong Kong.

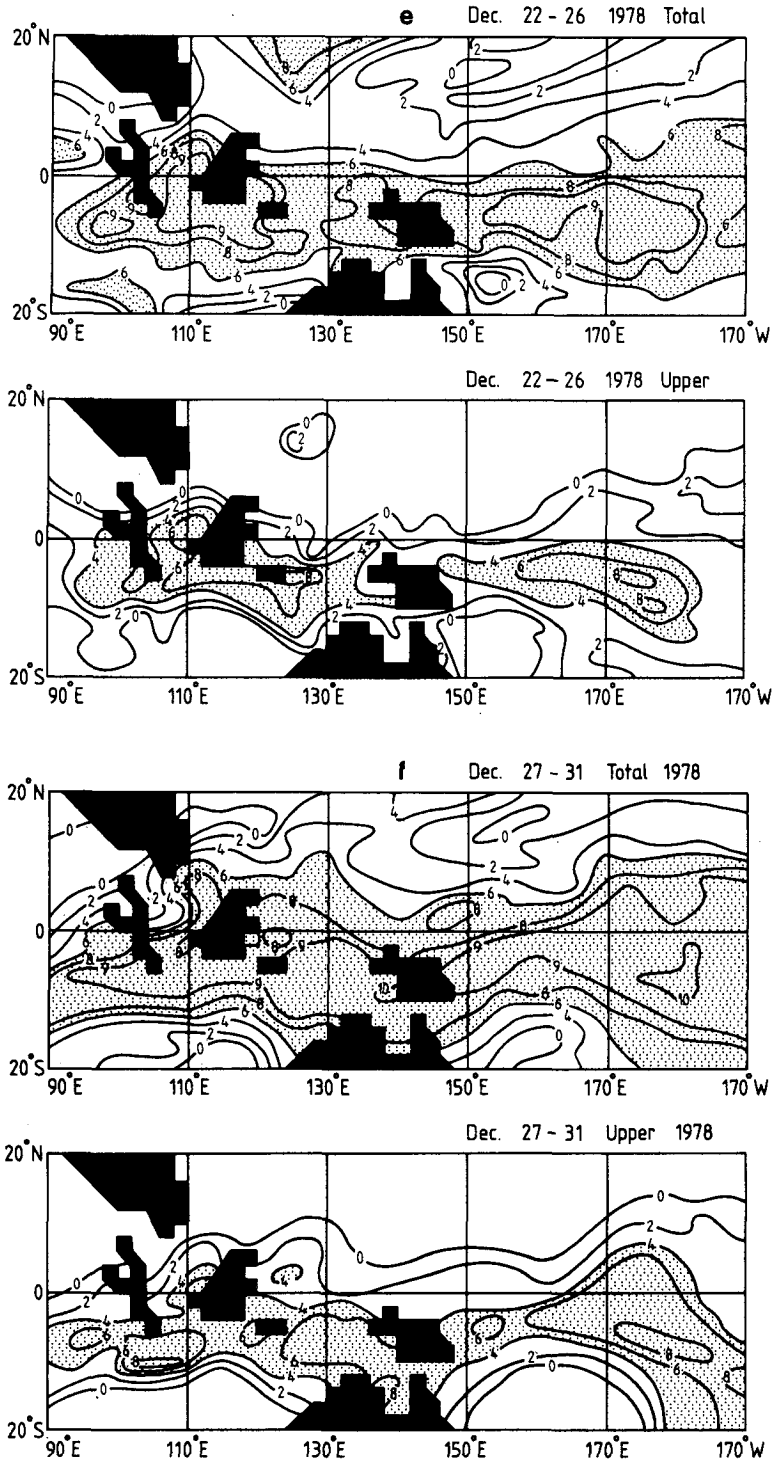

FIG. 1. (*Continued*)

For the purposes cited in the first section, a combination of the USSR radiosonde data, the aircraft data and the GMS photometry appears sufficient. The USSR ships provided observations every 6 h on a routine basis but every 3 h during a declared "intensive period." Consequently, the three ships provided a potential of excellent thermodynamic and dynamic coverage of the state of the South China Sea, immediately to the north of Kalimantan (Borneo). On the other hand, the GMS provided a wider overview of the region which, together with the land-based observations, allows the relationship between the USSR ship triangle and the ambient large-scale flow to be established. The

most important utility of the GMS is the provision of an effective radiating temperature structure of radiating surfaces from which estimates of the cloud-top heights of (optically thick) clouds can be determined. Thus the GMS is capable of determining *the extent, duration and top height* of the cloud. However, it provides no information regarding the thickness of the cloud or the height of its bottom. Fortunately, the structure of the lower part of the middle and upper tropospheric extended cloud decks were often obtainable from the research aircraft. Although neither the P3 nor the Electra carried dedicated radiation equipment, they operated (in the dropsonde mode) in the 500–400 mb range.

In summary, a combination of ship, aircraft and satellite data collected during WMONEX appears capable of providing an estimate of the four-dimensional structure of the extended clouds together with the evolving thermodynamic and dynamic structure of the atmosphere. However, as the aircraft were often deployed in other modes (e.g., low-level boundary layer missions as distinct from dropsonde flights) estimates of cloud base were only available on certain days.

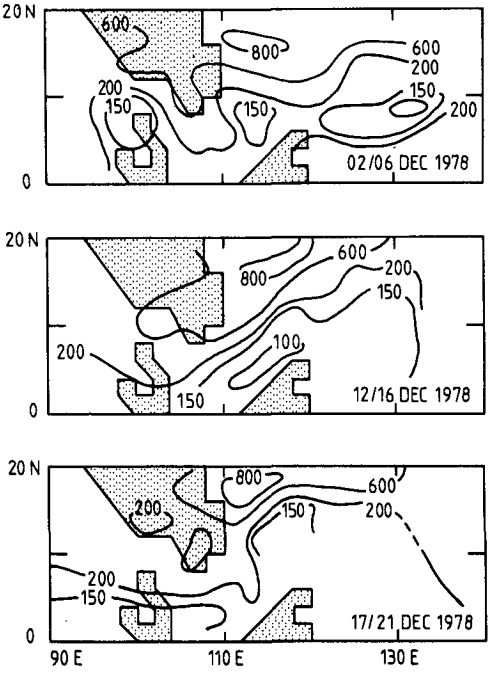

FIG. 2. Isopleths of cloud-top heights for the periods 2–6, 12–16 and 17–21 December 1978 (units: mb).

b. *Structure during Phase 1 of WMONEX*

A summary of the mean cloud structure during Phase 1 of WMONEX was presented in Fig. 1. The cloud distributions will now be related to the corresponding atmospheric structure using the serial atmospheric soundings from the USSR ships. For a detailed summary of the atmospheric state during WMONEX the reader is referred to the quick-look data set; in particular Sadler (1979).[4]

In a loose classification based on the location of the near-equatorial trough(s) to the west of 130°E, WMONEX may be divided into three major periods: 1–14 December, 15–22 December and 23–31 December. During the first period the equatorial trough resided for the most part in the Southern Hemisphere to the south of the main observing network in the South China Sea. Consequently, the disturbed regions were mostly to the south of Kalimantan in the Java Sea region. Although the 5-day periods of Fig. 1 do not precisely correspond to the first period (i.e., 1–14 December) the locus of the belt of extended upper level cloud may be seen to lie roughly along 5–10°S. Over the South China Sea, the area of upper level cloud northwest of Sarawak and Sabah appears more associated with dense "blow-off" from the diurnal towering cumulus over the heated land regions rather than organized disturbances. The surface and gradient level flows showed a general northeasterly stream with unimpeded cross-equatorial flow. During the second major period of WMONEX (15–22 December) the South China Sea was in its maximum disturbed state during Phase 1. The trough appeared north of Sarawak and Sabah with the surface flow generally offshore in the lower levels depending on the location of the disturbances. The final period (23–31 December) was similar to the first with the trough and disturbed region to the south of the equator. In summary, data from the WMONEX indicated an association between the fields of middle and upper level extended cloud and the disturbed regions of the WMONEX region. Extensive (and persistent) cloud decks also appeared upwind (i.e., relative to the middle-level wind structure) of the towering cumulus attached to the large island land masses[5] during undisturbed periods.

Moisture fields are shown in Fig. 3a. Time cross sections of daily mean relative humidity have been constructed for the three USSR ships for Phase 1 of WMONEX. During the first and last periods described above the region of maximum humidity is confined to the boundary layer with drier conditions aloft. Conversely, the middle period is characterized by a bimodal moisture distribution with a relatively dry lower tropospheric slab between 550 and 800 mb separated from a moist mid-troposphere by a large

[4] Sadler, J. C., 1979: Synoptic scale quick-look for Winter MONEX: December 1979. Department of Meteorology Tech. Rep. UHMET 79/02, Dept. of Meteorology, University of Hawaii, 3 pp.

[5] Similar features were observed during the Bay of Bengal experiment of Summer MONEX (July 1978). During periods of severe large-scale suppression GOES imagery indicated considerable cloudiness emanating from Burma. Aircraft penetrations identified the cloud as thick altostratus with characteristics similar to those noted above.

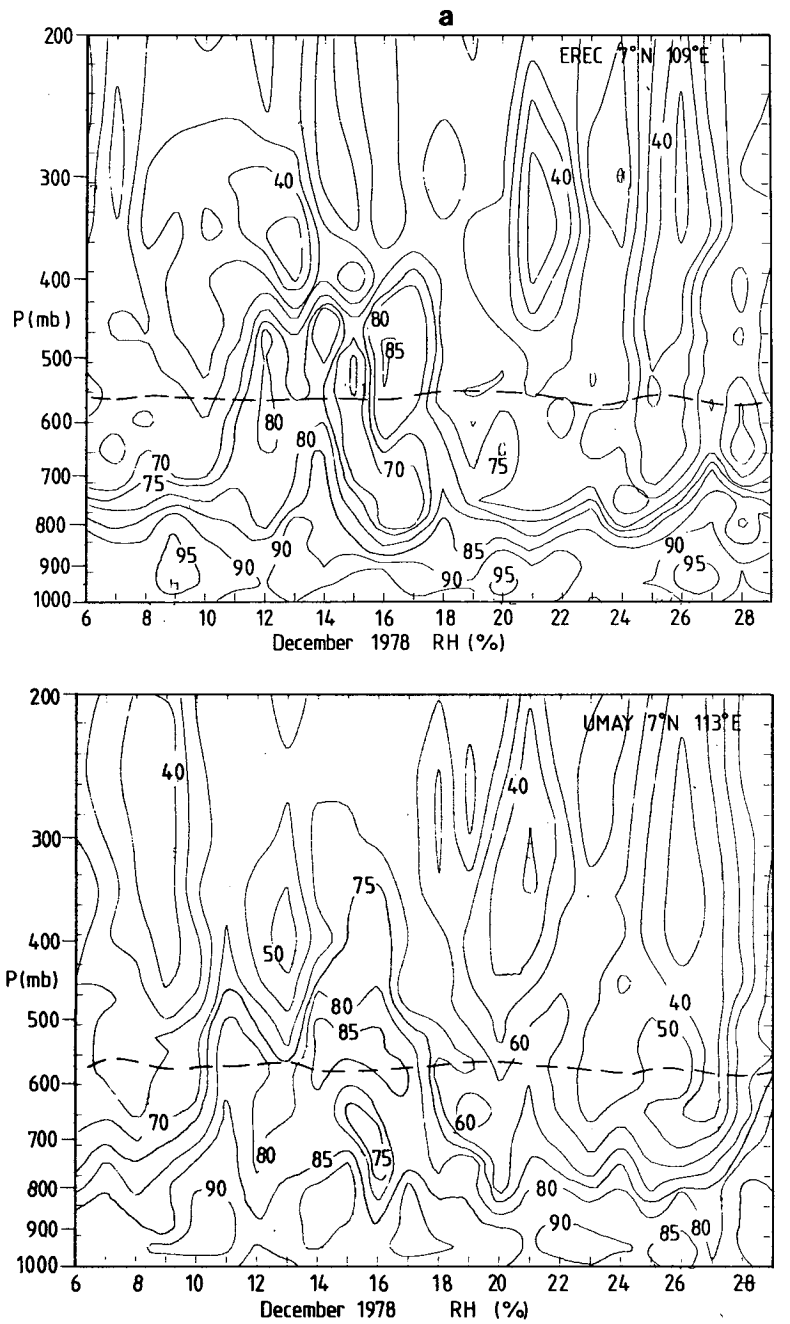

FIG. 3. (a) Time sections of relative humidity against pressure height for the three USSR ships located in the South China Sea during Phase 1 of WMONEX between 6–31 December 1978. The 0°C isopleth is shown as a dashed line. (b) As in Fig. 3a except for equivalent potential temperature (units: K).

humidity gradient near 550 mb. These features were common to all three ship locations. The humidity gradient was in the vicinity of the freezing level which is denoted by a dashed line in all three sections.

Companion θ_E sections are shown in Fig. 3b. The mid-tropospheric minimum (which generally characterizes tropical θ_E sections) appears in the vicinity of 600 mb for the undisturbed periods and closer to 800 mb for the disturbed periods. Values in the mid-troposphere are considerably larger during the disturbed period which with the smaller θ_E in the lower troposphere is consistent with the moisture distribution already discussed.

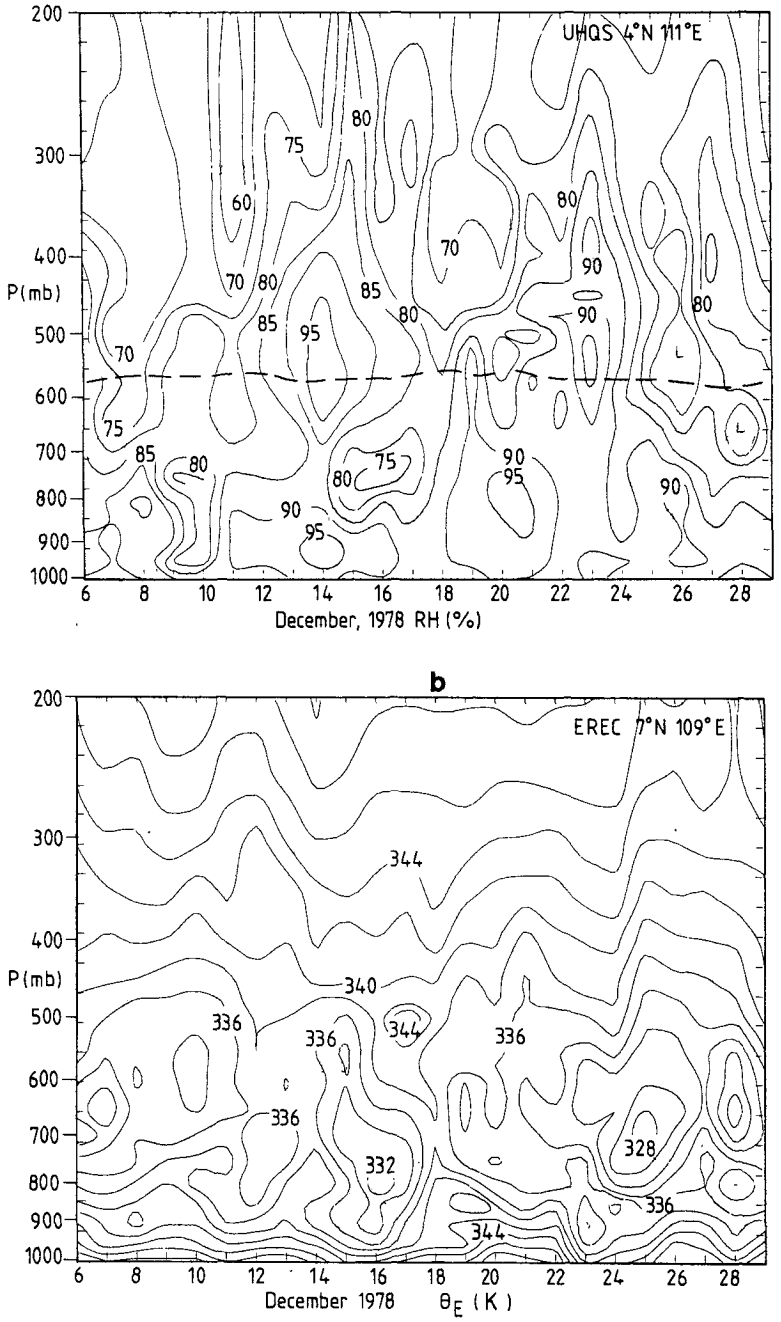

FIG. 3. (*Continued*)

Mean temperature and dewpoint profiles averaged over the USSR ship array are shown in Fig. 4a. The periods 7–9 December and 15–17 December 1978 are used to represent the first (undisturbed) and second (disturbed) periods, respectively. The dewpoint fields stress the nature of the undisturbed and disturbed periods; a dry middle and upper troposphere during the first period and a moist middle troposphere during the second above a relatively sharp moisture gradient. Interestingly, the temperatures in the boundary layer are slightly warmer in the mean (~1°C) during the first period although the temperature profiles are almost identical in the middle troposphere. Beyond this only the moisture structure is significantly different.

The corresponding equivalent potential temperature profiles are shown in Fig. 4b. Calculated for the same periods, the θ_E profile for the disturbed period shows a 5 K excess in the middle troposphere with slightly lower values in the lower

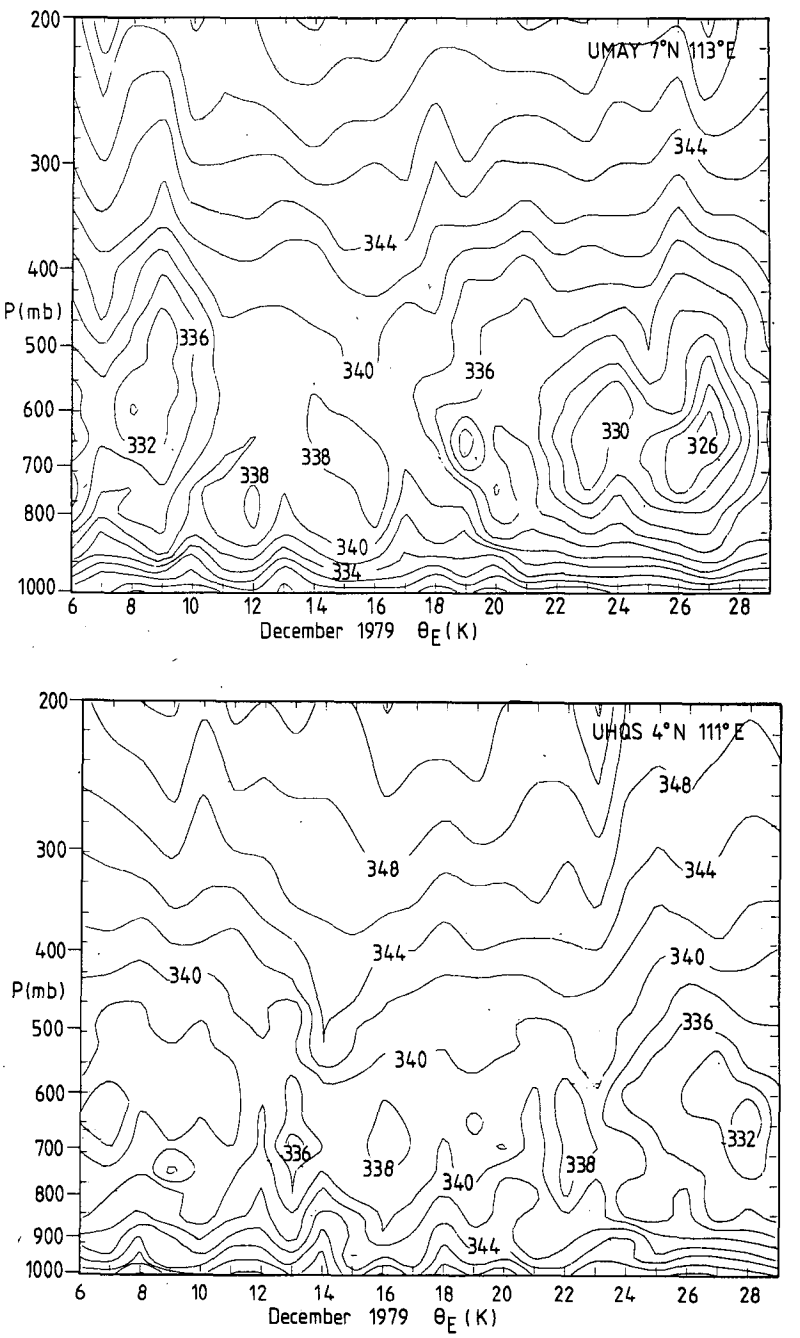

FIG. 3. (*Continued*)

troposphere. The θ_E profiles are consistent with temperature and humidity distributions of Fig. 4a. It is interesting to note that the θ_E profiles differ greatly from those obtained in the *convective* areas of tropical disturbances. Plotted with the mean WMONEX data in Fig. 4b are the convective and suppressed θ_E profiles obtained from the 1957 and 1963 research cruises of the *Crawford* to the east of Barbados in August.[6] The suppressed curve possesses a considerably lower mid-tropospheric

[6] Based on data summarized by N. Laseur, M. Garstang and C. Aspiden, 1967: Equivalent potential temperature as a measure of the structure of the tropical atmosphere. Final Report, U.S. Army ERDL, No. 67-10, 44 pp.

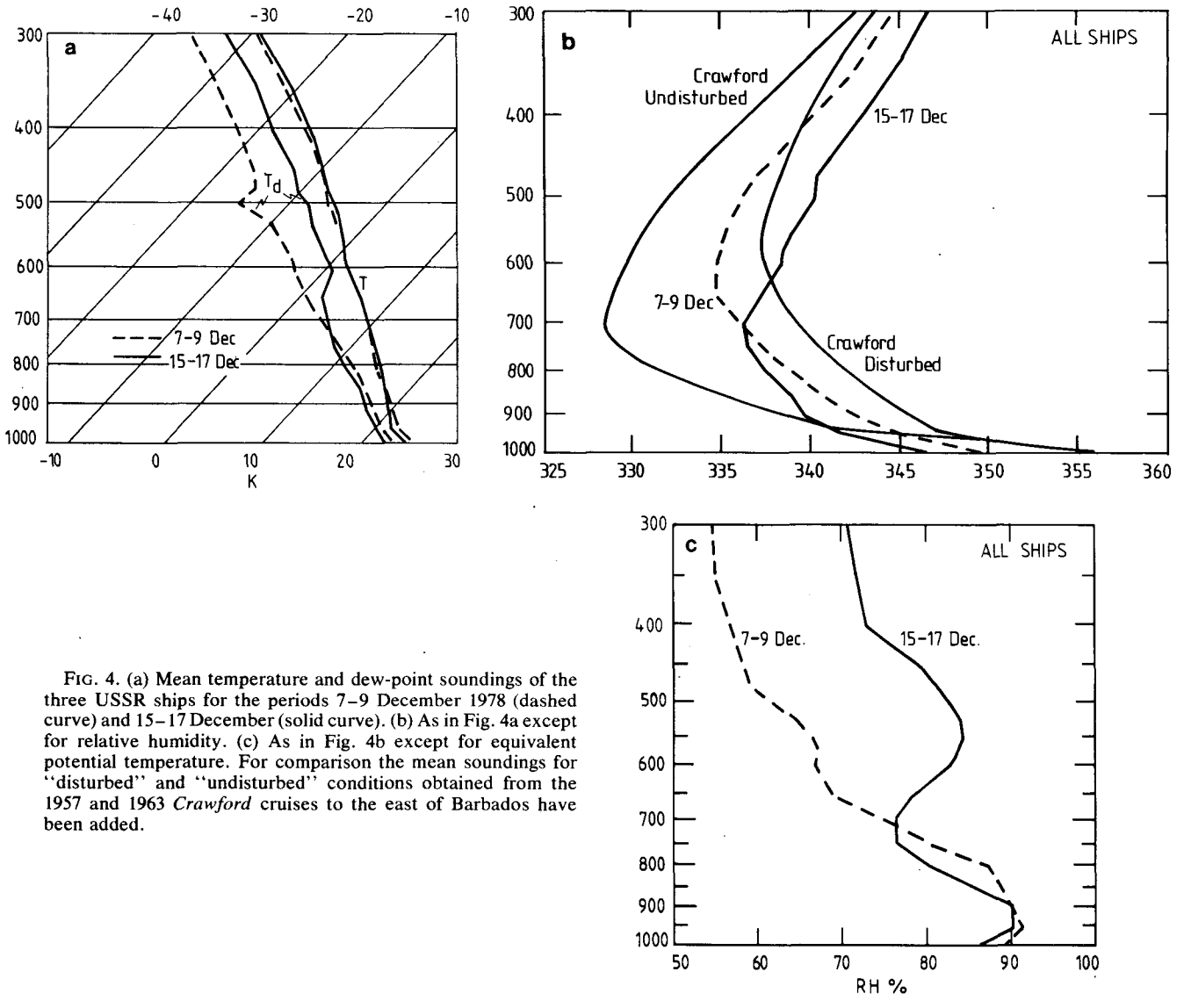

FIG. 4. (a) Mean temperature and dew-point soundings of the three USSR ships for the periods 7–9 December 1978 (dashed curve) and 15–17 December (solid curve). (b) As in Fig. 4a except for relative humidity. (c) As in Fig. 4b except for equivalent potential temperature. For comparison the mean soundings for "disturbed" and "undisturbed" conditions obtained from the 1957 and 1963 *Crawford* cruises to the east of Barbados have been added.

minimum than for either period during WMONEX. In fact, the WMONEX first-period curve appears to match the *Crawford* convective profile quite well. What is most evident is the extremely high values of the WMONEX disturbed curve in the middle and upper troposphere compared to the convective curve and the considerably lower values in the lower troposphere. The implication is that the soundings of the three USSR ships during the period from 15–17 December 1978 were not in the convective region of the disturbance *but were in the outflow region dominated by the middle tropospheric extended cloud.*

Fig. 4c shows the mean relative humidity sections for the two periods. The bimodal moisture distribution is particularly evident in the 15–17 December mean profiles.

c. Case study—17 December 1978

As emphasized earlier, middle and upper tropospheric extended clouds appeared as the most common species in the main observational region of WMONEX during the second period (i.e., 15–22 December 1978) when the locus of disturbances temporarily established itself in the Northern Hemisphere. During this period the cloud was densest off the Sabah and Sarawak coasts and generally extended north and west of the disturbed region for hundreds of kilometers.

A characteristic day of the period was 17 December which corresponded to the second day of a 2-day "vortex mission"[7] which employed the two principal research aircraft operating at maximum altitude in the dropsonde mode. The aircraft flightpaths complemented the USSR ship array and operated (at least during part of the mission) in the vicinity of the Bintulu radar. Other missions were planned and implemented during WMONEX during active periods with extensive middle decks (e.g., the Java Sea mission of 6 December) but they did not have the advantage of being supported by the WMONEX composite observing network in the South China Sea.

Figs. 5a and 5b show the visible (portion of the full disc picture) and infrared (section of the Mercator section)[8] GMS data for 0600 GMT 17 December. Three principal areas of bright upper level cloud may be discerned. For the present purposes the most important area is that occupying the South China Sea. A second area exists over the Java Sea which is typical of the cloud extent in that region during the first weeks of WMONEX (see Figs. 1a and b). A third area is evident west of Sumatra and is associated with a propagating disturbance which formed to the west of the island. Overall, the middle and upper level extended cloud is so extensive that it occupied over 50% of the area bounded by 105°E, 115°E, 7.5°N and 5°S, i.e., an area in excess of 6×10^5 km^2.

To provide an indication of the height of the cloud deck, isopleths of cloud top pressure (mb) are drawn on Fig. 5b. The data obtained from the GMS shows the cloud deck to the northeast of Borneo to be above 200 mb. Unfortunately, data was not available for the Java Sea region but comparisons using the grey calibration scales indicates similar cloud-top temperatures.

Fig. 6a shows the aircraft tracks and cloud fields observed from the aircraft. Times (local) at which the aircraft reached certain points along the tracks are marked. Preliminary dropsonde data (kt) for the 950 mb level are plotted for both the P3 and Electra (dashed and solid lines, respectively) along their flight paths. The USSR ship winds are also superimposed. A weak vortex is discernible at 950 mb in the vicinity of 7°N, 114°E as noted by Greenfield and Krishnamurti (1979) in their analysis. Two major cloud structures were identified from the aircraft. These were the extensive upper and middle-level cloud shield discussed earlier (denoted by light stippling) and the regions of active convection (shaded) which corresponds to either P3 radar echoes or aircraft penetrations. Hatched areas denote regions of precipitation observed to emerge from the base of the middle-tropospheric extended cloud deck or encounters by the aircraft during penetration of ice particles or supercooled water droplets.[9] Note that only those regions of precipitation well removed from the active convection are shown. In fact, in all cases of observed stratiform precipitation the lower troposphere possessed little or no cumulus activity except for scattered stratocumulus. In summary the regions of extensive precipitating middle and upper level extended decks possessed indications of complete suppression, a point previously noted in Fig. 4a.

The base of the extended cloud, away from the regions of convection, appeared to be in the vicinity of the freezing level. The estimates obtained from the aircraft flight-level information were substantiated by the USSR ship data seen in Fig. 3. Fig. 6b shows a composite of the dew-point depression ($T - T_d$) obtained from the research aircraft flight-level information, dropsonde data, USSR ship rawinsondes and the convection upper air sounding network. Two major regimes are evident. The first, which is representative of the majority of the tropical atmosphere away from the cloudy regions of Fig. 5, shows a dew-point depression in excess of 10°C. The second regime, which mirrors almost exactly the extent of the cloud shield noted in Fig. 6a, indicates near saturation in the vicinity of the 500–600 mb levels. Most importantly, Fig. 6b indicates that the base of the extended cloud deck extends at least 700 km from the major convective region with a thickness of some 300 mb.

The flight level and 500 mb winds are indicated on Fig. 6c; the data source and precise level being identifiable from the legend. The flow emerges from Borneo in a generally east-southeasterly direction turning to southwesterly around the ridge extending across the South China Sea. Most importantly, the middle and upper level cloud shield extends downwind from the convective source regions and is thus consistent with the larger scale flow.

Fig. 7 indicates the character of the subcloud layer below the extended clouds. Shown are a sample of the dropsonde profiles obtained from the research aircraft during the mission. Profiles A and B (which refer to points marked on Fig. 6a) indicate the characteristics of the vertical distribu-

[7] Greenfield and Krishnamurti, (1979) present a short summary of the various WMONEX missions and the data available from them. They present circulation charts for 17 December 1978 at 950, 850 and 700 mb using the dropsonde data as examples of the aircraft data.

[8] A common area is outlined on the full disc and mercator projections to facilitate comparison.

[9] Specific identification of the ice crystal form and size distribution must await analysis of the cloud physics experiment. Tentative inflight identification was graupel. Supercooled water droplets were associated with icing and easier to identify.

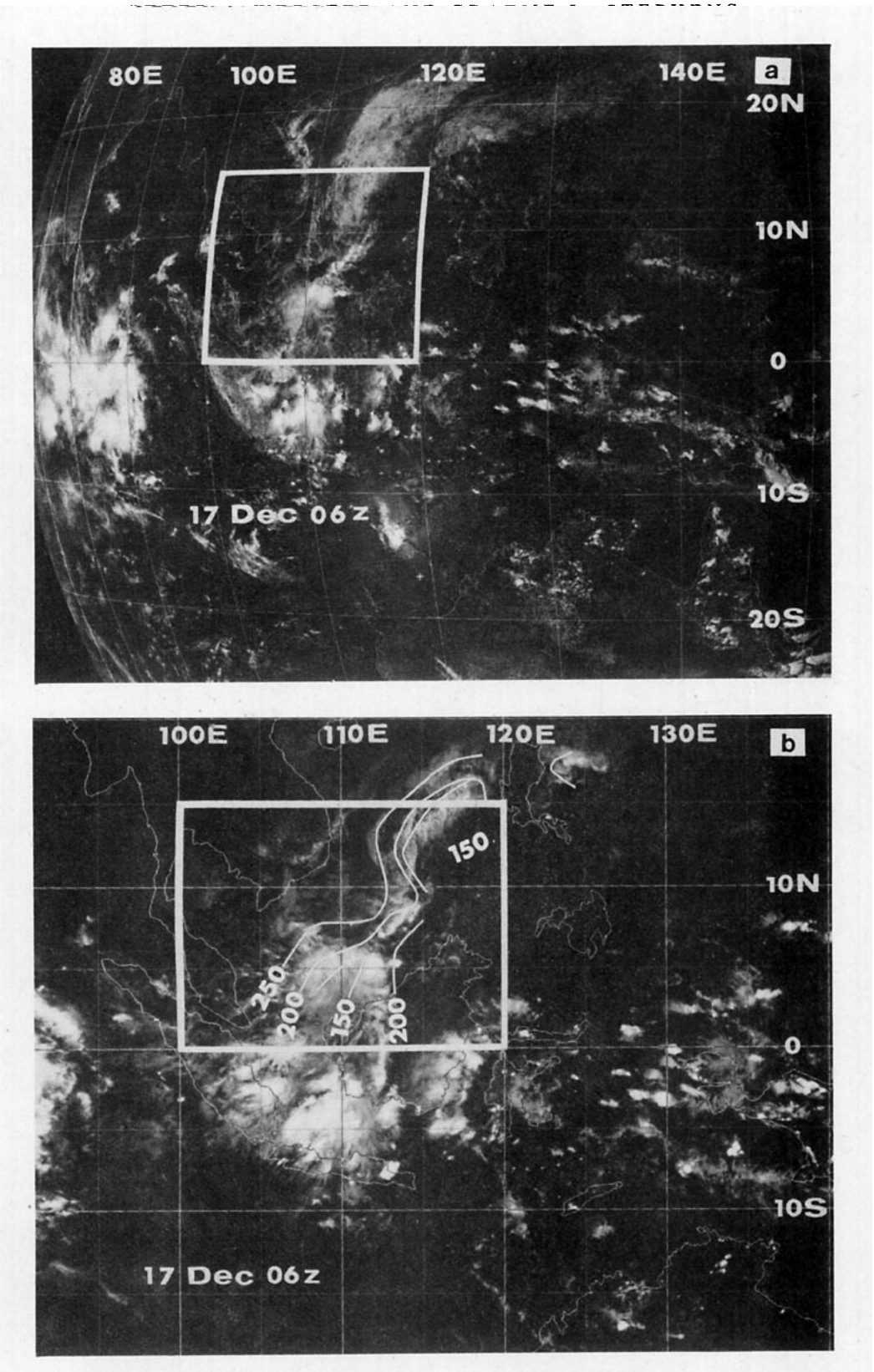

FIG. 5. (a) Visible GMS 1 imagery for 0600 GMT, 17 December 1978, from full disc image. (b) Infrared GMS 1 imagery for 0600 GMT, 17 December 1978, from Mercator projection image. Common area with Figs. 5a and 6 is bordered in white. Isopleths of cloud-top height are superimposed.

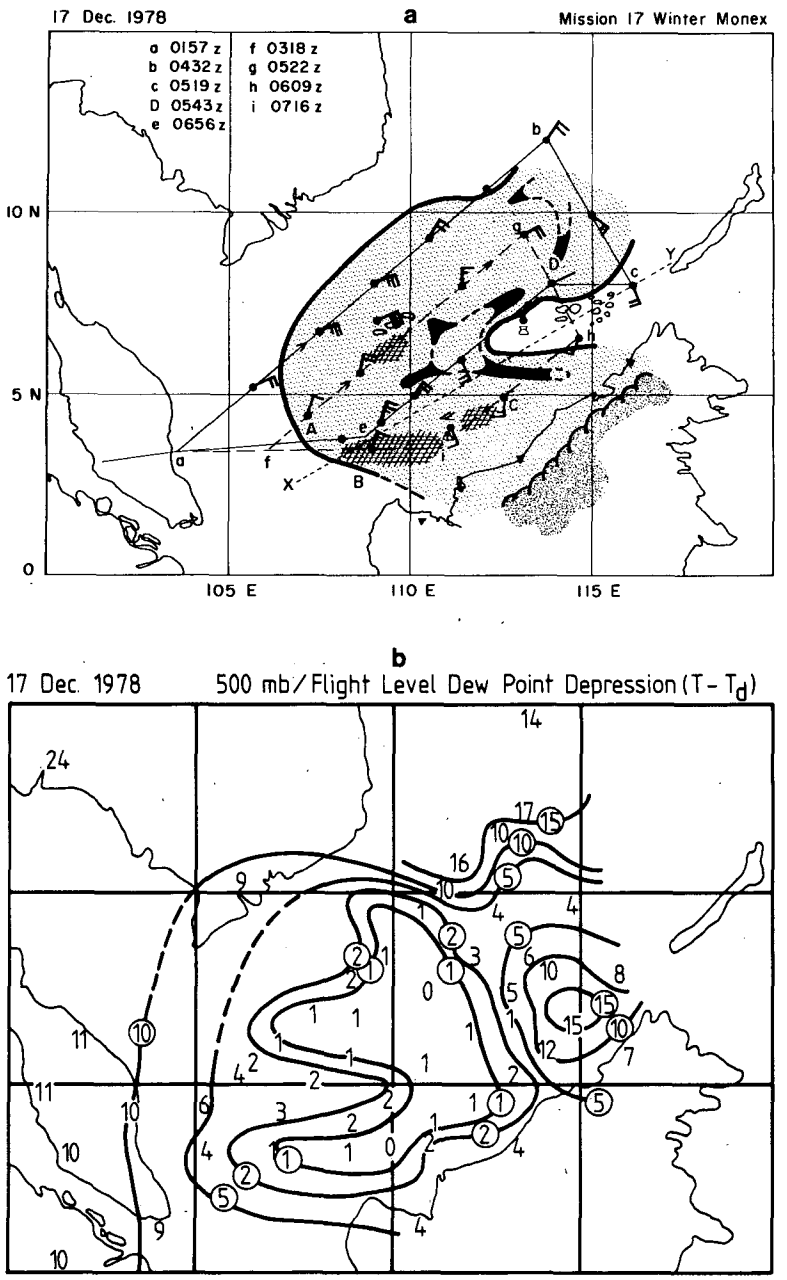

FIG. 6. (a) Flight-level visual record of mission 17 of the Winter Monsoon Experiment, 17 December 1978. Flight paths are shown as thin solid lines (NOAA P3) and thin dashed lines (NCAR Electra). 950 mb Electra and P3 dropsonde winds and surface observations are shown in conventional format. Light shading shows upper level cloud area. Dark shading denotes convective regions. Hatched area indicates observed extended cloud precipitation or graupel. Letters A–D refer to location of dropsondes shown in Fig. 7. (b) Distribution of dewpoint depression of mission 17. Data base includes regular radiosonde data, USSR ship data and the P3 and Electra flight-level record. (c) Composite middle tropospheric wind data. Data base is as in Fig. 6b and analysis refers to 500 mb.

tions of T and T_d beneath the extended decks. Both A and B indicate an extremely moist upper and middle troposphere and a dry lower troposphere above a shallow, moist boundary layer lying below a weak inversion. It should be noted that A and B show strong similarity to the USSR ship data noted in Figs. 3 and 4a. Such structures are consistent with the suppressed lower troposphere noted earlier.

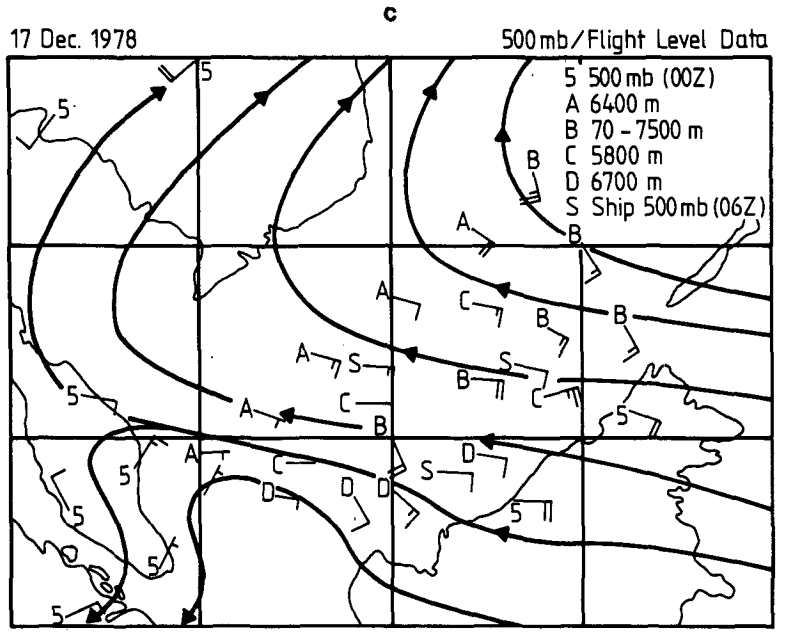

FIG. 6. (*Continued*)

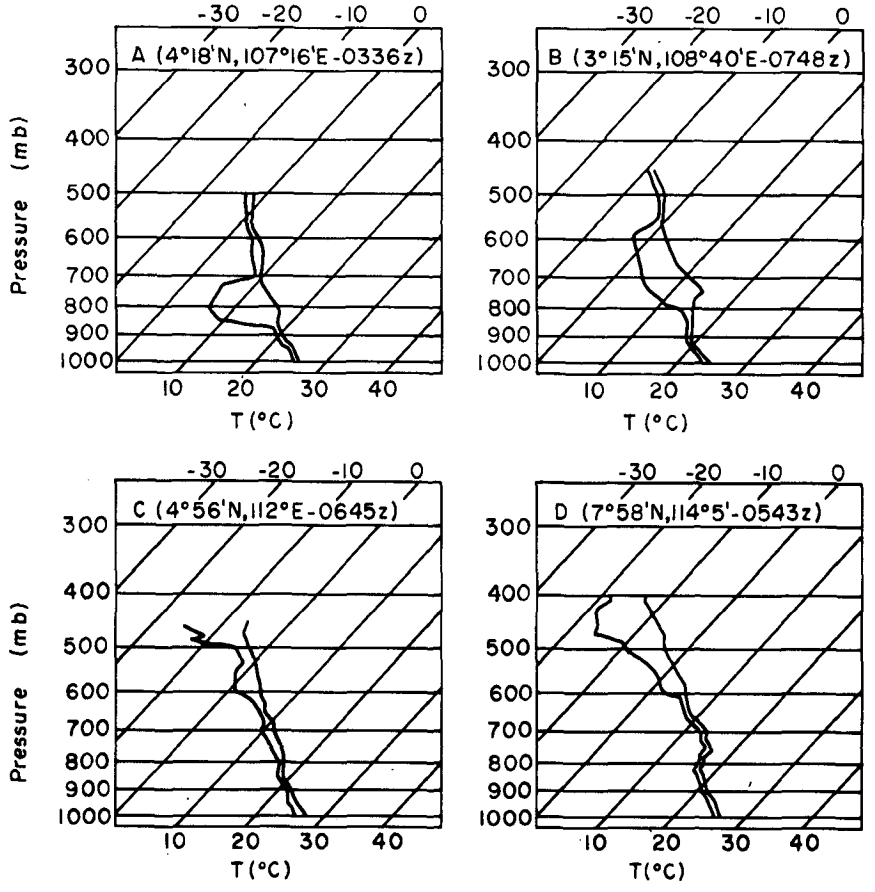

FIG. 7. Dropsonde temperature and dew-point profiles for 17 December 1978. Letters refer to locations marked on Fig. 6a.

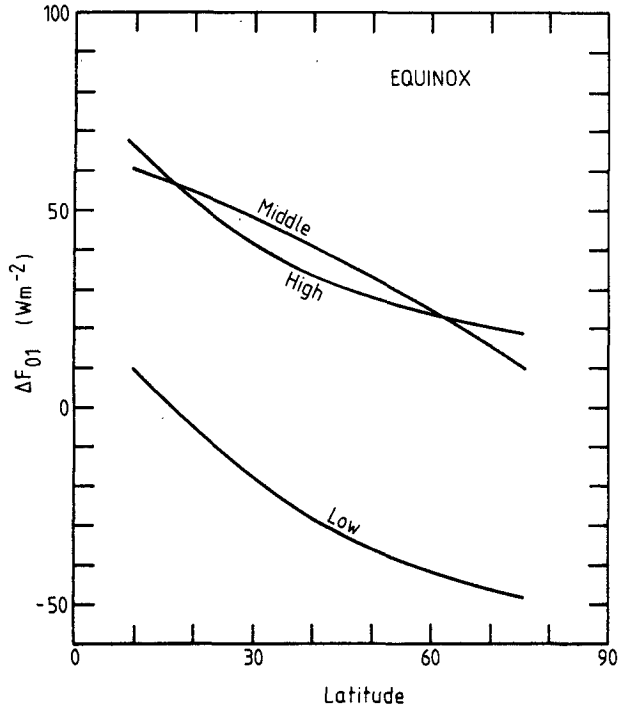

FIG. 8. Variation of net radiative flux is an atmospheric column between totally covered and clear skies as a function of latitude for three cloud species. Calculations from the static radiative transfer model of Stephens and Webster (1979).

Shown for contrast, the profiles C and D indicate conditions nearer to the regions of penetrative convection noted in Fig. 6a.

4. Radiative properties

An indication of the potential importance of the middle and upper level extended clouds, viewed from a radiative perspective, may be gained from Fig. 8.[10] Shown is the variation of the *difference* of the net radiative flux of the atmospheric column between totally covered and clear skies of low, middle and high clouds plotted as a function of latitude. Two points are apparent. First, the magnitude of the differential net radiative flux for the middle and high cloud is considerably greater than that for low cloud. Second, the magnitude of the net radiative flux is a maximum in low latitudes. Most importantly, the net radiative difference between clear and totally covered sky of (say) 10°N is of the same magnitude as the corresponding latitudinal gradient of net flux divergence. In fact, from Fig. 1, an extremely strong gradient in radiative flux divergence would be expected in the vicinity of the edge of the equatorial upper level cloud band.

[10] Calculations were made using the radiative transfer model developed by Stephens and Webster (1979). The properties of the three species are listed in their Table 1.

With the cloud and atmospheric structure obtained from WMONEX it is possible to calculate the radiative heating profiles in the vertical for various cloud structures. To obtain the profiles we use the relatively sophisticated multiple-scattering radiative transfer model (Model A) of Stephens (1978) which calculates both long- and shortwave fluxes through a cloudy atmosphere. The atmosphere is composed of 50 mb slabs extending from the surface to 100 mb and the basic atmospheric state was chosen to match the mean South China Sea conditions (see Fig. 4). The cloud portion was assumed to be in the ice phase and the thickness determined from the satellite-derived cloud-top height. The cloud bases were chosen to match those observed by the research aircraft. The particle size distribution of the crystal cloud employed in the calculations was taken from the measurements of Cox and Griffith (1977).

Figs. 9a and 9b show the vertical distribution of the infrared heating rate (solid curve), the shortwave heating rate (dashed, and calculated using daily average insolation) and the total radiative heating rate for two clouds (shaded area) occupying the 600–200 mb slab, which matches the observations, and the 350–200 mb slab calculated for comparison. In each case, the effect of the cloud deck is dramatic in both the long- and shortwave regions. The shortwave radiative heating is due to the effective absorption of solar radiation by both cloud material and water vapor. The infrared heating at the base of the cloud underlines the effectiveness of an upper deck to absorb the ingoing longwave radiation emanating from lower, warmer regions, i.e., both systems are optically black. The longwave structure in the upper portion of the cloud represents the distinct cooling to space.

The *total* effect of the radiative heating is to produce substantial heating in the lower part of the deck (~20 K day^{-1}) with cooling at the top (~ −15 K day^{-1}). Such a result is in sharp contrast to the mean tropical heating rates of Dopplick (i.e., weak net cooling throughout the atmospheric column irrespective of cloudiness) but in agreement with Albrecht and Cox (1975) and Cox and Griffith (1979).

Integrating the heating with height shows for both cases a net *heating* throughout the slab and, incidentally, through the entire depth of the atmosphere. Considerable diurnal variation is also implied. During nighttime, the shortwave contribution is absent and the total heating curve matches the longwave curve. Integrating once again with height, the total heating shows *small net cooling* both throughout the column and in the cloud. Such radiative heating or cooling would constitute *part* of the total diabatic heating function which would

include the Leary and Houze functions of evaporation and melting cooling at and below the base of the cloud deck.

5. Extensions and conclusions

a. Summary

Using data obtained from both the conventional and special observing platforms of the WMONEX, a number of general statements may be made regarding the cloud structure. These are summarized as follows:

1) The predominant cloud species during December 1978 in the Indonesian and South China Sea region was extended upper and middle troposphere cloud layers or shields. Within 10° of the equator there existed a strong positive correlation between total cloud and high cloud. The high cloudiness values which lasted through the 5-day average periods indicated substantial persistence of coverage.

2) The majority of the middle and upper level cloud appeared to be associated either with disturbances along the equatorial trough(s) or with the diurnal thunderstorms which appear as recurring features over the large islands of Southeast Asia and Indonesia. The upper level cloud shields often extended laterally to 1000 km from identifiable convective source regions.

3) GMS data indicated cloud-top heights above the 200 mb surface. Research aircraft data indicated bases in the vicinity of the 500–550 mb levels (or near the −5 to 0°C isotherms). Dropsonde data indicated warm and dry conditions below the cloud deck above a moist boundary layer surmounted by a weak inversion. On all occasions there was little or no evidence of convective activity in the low troposphere below the extended cloud away from the convective source regions. Radiosonde data from the USSR ship triangle corroborated the research aircraft observations as well as providing limits on cloud longevity and spatial extent.

4) In the disturbed situation from 15–17 December 1978, large upper and middle level cloud decks were constant features over the USSR ship array, indicating a disturbance longevity substantially greater than the well-documented GATE disturbances.

5) Precipitation was observed to fall from the base of the upper and middle level extended cloud system in locations well removed from the convective source region. The cloud systems

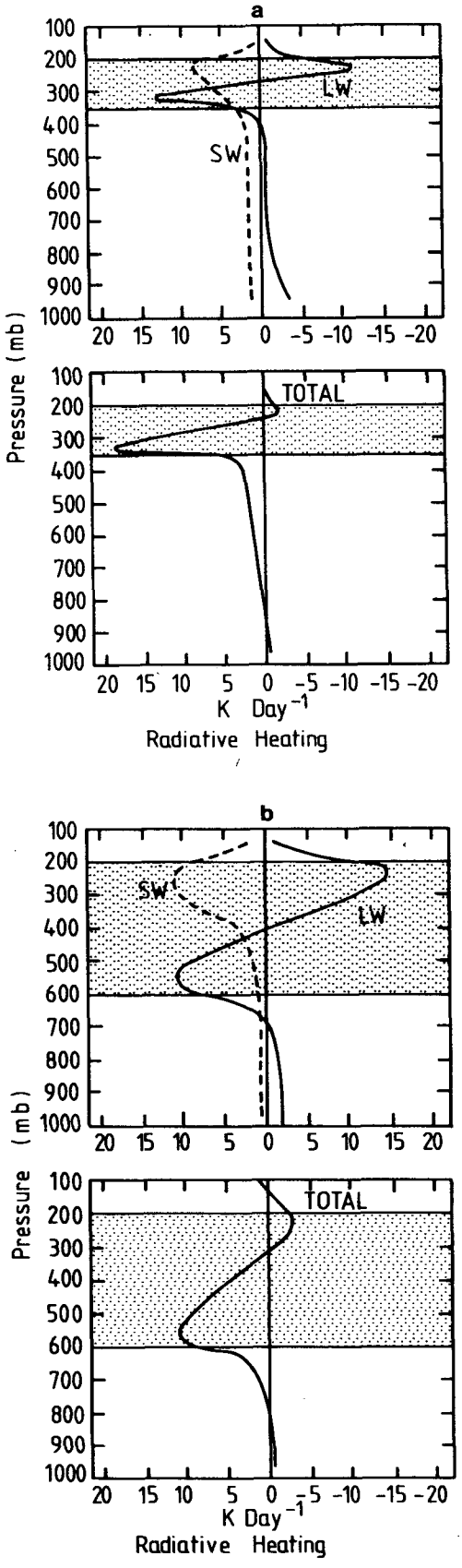

FIG. 9. Vertical distribution of radiative heating in the visible (dashed) and infrared (solid) relative to a cloud slab (a) between 200 and 350 mb and (b) between 200 and 550 mb.

were observed to have the form of nimbostratus decks. Cloud-base penetrations by the research aircraft indicated supercooled water droplets and (probably) graupel. Precipitables were observed on scales which varied from tens to hundreds of kilometers.

Using the data collected from the WMONEX which defined the atmospheric and cloud structure transfer models, developed in earlier papers, a number of inferences could be made regarding the interaction of extended clouds and the radiative field. These were as follows:

1) Dense optically black middle and upper level cloud impart a significant perturbation on the net radiative flux of the atmospheric column. Because of the areal extent and persistence of the extended clouds they probably form the major perturbation to the near-equatorial radiation balance.

2) Substantial horizontal gradients in the net radiative flux of the atmospheric column may be expected between the equatorial trough region and the clearer regions to the north and south.

3) Optically black middle and upper tropospheric cloud decks appear as major perturbers of the vertical radiative heating profile. In sharp contrast to the Dopplick (1963) profile, radiative transfer calculations indicate substantial heating at the base of the cloud deck and a larger cooling to space at the top of the cloud. A heating rate differential of nearly 30°C day^{-1} was estimated. A large diurnal variation in net radiation was shown to exist which would be caused by the diurnal variation of absorption of incoming short wave radiation in the upper portion of the cloud.

b. Processes and mechanisms

Ideally, at this stage, one would hope to describe a physical process or a chain of processes which would aid in understanding the phenomena noted above. However, prior to undertaking a considerable modeling effort (see below) we are forced to test the observations against earlier results of both a theoretical and observational nature in an attempt to trace either consistency or inconsistency in the logic. With this methodology we will discuss the three questions raised in the Introduction.

1) SOURCE OF THE EXTENDED CLOUD

There appeared abundant evidence during WMONEX of the extended cloud being associated with large-scale convection. In all cases of extensive shield cloud either a circulation feature or convective event associated with the diurnal heating of the islands was evident. Overall there appeared to be no evidence of synoptic scale uplift with which one may often associate midlatitude decks.

2) CLOUD MAINTENANCE; LONGEVITY AND EXTENT

If extended clouds are at least initially cumulonimbus debris, a knowledge of particle fall speed, evaporation rate, vertical motion and total horizontal wind speed would yield an estimate of the horizontal extent of the cloud system. That is, if we hypothesize that there is no diabatic heating within the anvil the estimate of extent reduces to knowing the fall time from ejection to evaporation. The following estimates are based on the *conservative* assumptions that the environment of the source region is *non-subsident* with a zero vertical velocity component, possesses a relative humidity of 75% (see Fig. 3) and that the emitted particles are ice crystals which originate in the source region near 350 mb. Using the terminal velocity estimates of Heymsfield (1972) for the slab 350–550 mb and taking into account the evaporation of the ice near the melting zone, horizontal cloud deck extents were calculated to be from 150 km for 0.5 mm bullets to 200 km for 0.5 mm plates if a horizontal wind speed of 12.5 m s^{-1} was assumed throughout the slab. That is, in the *absence of external heating* (i.e., utilizing a "quiescent debris" model), the horizontal extent of the cloud decks would be < 200 km.

The quiescent debris model utilizing conservative assumptions aimed at *maximizing* the cloud horizontal extent, underestimates the real extent by a factor of three or four. Thus either the basic premise of the model is incorrect or an approximation ill-founded. In any event, a mechanism is required to increase the suspension time of the cloud ice-particles by a considerable amount. In fact, if the size distribution of the particulates was correct, then a net upward vertical velocity of $\sim$0.30 m s^{-1} (i.e., the difference between the fall speed necessary to produce the required suspension and the ice-particle terminal velocity) either as a mean uplift or as a rectified effect of smaller scale processes would be required to produce an extended cloud of observed proportions.

3) DIABATIC HEATING

In order to account for the longevity of the cloud debris diabatic heating must be invoked. Two forms are applicable; latent and radiative heating.

The latent heating is associated with phase changes within and below the cloud deck. As noted earlier for the GATE systems (Leary and Houze, 1979) melting produced cooling at the base of between 1 and 7 K h^{-1} while evaporation provided cooling of 0.2–6 K h^{-1} below the cloud deck. Five case averages were 3.6 and 2.2 K h^{-1}, respectively. The estimates refer to rather intense systems exhibiting anvil precipitation of between

1 and 10 mm h^{-1} within 100 km of the convective region. Such systems are probably much more intense than the WMONEX disturbances. Besides the question of anvil scale discussed earlier, it seems that the extended cloud precipitation observed during WMONEX was considerably weaker than noted in the GATE system. However, the GATE systems of Leary and Houze are probably the best-documented systems and at least allow the role of radiation to be assessed in conditions of *intense* convection and anvil precipitation.

The radiative function results from cloud-radiative feedbacks. The form of the function is summarized in Fig. 9 and shows many of the characteristics observed by Albrecht and Cox (1975) and Cox and Griffith (1979).

An important aspect of the total diabatic heating function is that it is a composite of functions of different signs. Latent effects tend to cool the lower part of the cloud (melting) and the subcloud layer (evaporation) and to heat the interior of the cloud. Conversely, the radiative processes tend to warm the lower part of the cloud (absorption of upcoming infrared radiation) and to cool the top (cooling to space, which is emphasized at nighttime due to the absence of solar radiation). Consequently, *latent heating effects tend to stabilize the thermal structure of the cloud, whereas radiative processes tend to destabilize the thermal structure*. The important factor lies in the relative magnitude of the two component functions. Radiative processes will tend to remain constant for the same cloud structure; the magnitudes depend primarily on the cloud thickness (i.e., its optical blackness) and the cloud-base height. On the other hand, the magnitude of the latent effects are strong functions of the intensity of anvil precipitation which, in turn, depends on the intensity of the disturbance, the stage of its lifecycle and the distance of the atmospheric column from the convective source.

With these criteria in mind, it would appear that radiative processes will possess a varied importance depending on the disturbance in question or the particular location within the disturbance or its outflow region. For an extremely vigorous disturbance such as Leary and Houze's case 1, which exhibited anvil precipitation of 8–9 mm h^{-1}, radiative processes will almost certainly be of secondary importance in the total diabatic heat balance of the column. For disturbances 2 and 4 (precipitation rates of 0.3 and 2.3 mm h^{-1}, respectively) radiative heating at the base of the cloud tends to approach magnitudes which are similar to that of the latent heating due to melting. This is shown schematically in Fig. 10 where profiles of the two diabatic heating rates are drawn. For the average Leary-Houze disturbance the magnitude of the

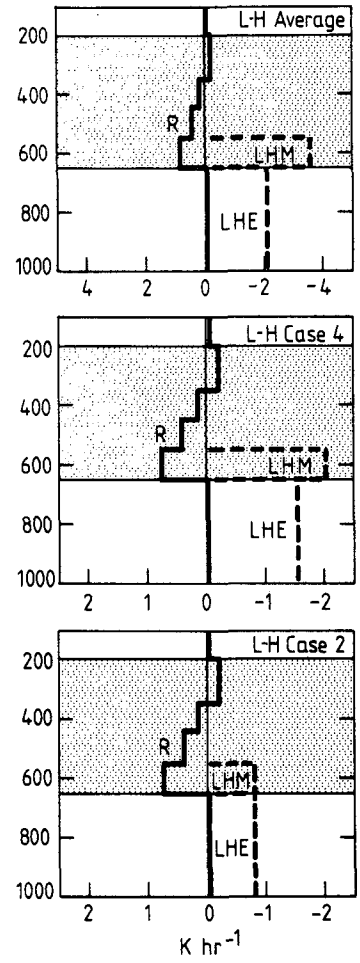

FIG. 10. Schematic comparison of diabatic heating rates for the average disturbance of Leary and Houze (1979) (upper) and their cases 4 (middle) and 2 (lower panel). R refers to radiative heating, LHM to cooling due to melting and LHE to cooling due to evaporation. Cloud slab extends from 200–650 mb. Note scale change between upper and lower two panels. Units are K h^{-1}.

radiative heating is only 11% of the total cooling for melting and evaporation. For case 4 it accounts for 17%, whereas for the weakest example of the set, case 2, the magnitude has risen to 33%. Thus with decreasing intensities the effect of radiative processes gain in importance.

The apparently smaller precipitation rates of the WMONEX disturbances, observed in discrete regions well away from the convective source region (see Fig. 7), are perhaps less intense than Leary and Houze's disturbance 2. Unfortunately, the WMONEX estimates depend on visual observations of the precipitation and quantitative assessments must await analyses and publication of the research aircraft and land-based radar data. However, extrapolation of the analysis of Fig. 10 to weaker disturbances with smaller outflow region precipitation allow some indication of the role

radiative processes play in the disturbances observed during WMONEX. Considering the limiting case when precipitation processes are absent from the extended cloud, radiational heating at the base of the cloud must become the dominant diabatic heating form and destabilization preponderate. The preferred scale of convective overturning resulting from the destabilization would be of the scale of the extended cloud thickness itself (i.e., ~7–10 km) which would produce regions of precipitation from the anvil. The undulations which were observed to occur well below the mean base height of the deck in the region of precipitation are consistent with the formation of melting regions of the aggregated crystals below the freezing level. That such crystals occur is substantiated by the research aircraft observation of graupel in passages through the precipitating zones. A similar latent heat format to that of Leary and Houze, but substantially smaller in magnitude, follows with cooling below the cloud deck caused by evaporation of the precipitation. There was some evidence of evaporation during WMONEX with the light precipitation falling from the undulations of the cloud deck in the form of virga.

Besides providing a potential for precipitation formation of the extended cloud at great distances away from the convective source, it should be noted that the radiative effects themselves constitute a *net* warming of the cloud deck during the day which would partially maintain the cloud system via lifting. Such heating is in addition to the latent heating from within the cloud.

Whether or not the extended cloud breaks into *visible* cellular structure following the initiation of the stabilizing convection within the extended cloud depends on the ability of the residual ice crystals to withstand sublimation within the enhanced subsidence between the precipitation regions during their descent to cloud base. Furthermore, it is not possible at this stage to understand why precipitation was observed to occur over a large variety of scales (see Fig. 6) when the initial convection would possess a preferred scale.

The solution of these problems may be connected with the reemergence of the latent heating (or cooling) within and below the cloud after the advent of precipitation. However, further speculation should await the development of appropriate models or the diagnosis of more specialized data than was used in this study.

c. *Concluding remarks*

A varying degree of importance has been suggested for radiative processes in the near-equatorial regions. Calculations suggest that from a purely radiative viewpoint, the existence of vast decks of middle and upper extended clouds (see Fig. 1) must have a large influence on the radiative balance of the tropical atmosphere. The role of radiation in the maintenance of features close to the convective source appeared to depend on the strength of the disturbance itself. In systems with vigorously precipitating anvils latent effects clearly dominate. However, with smaller precipitation it appears that radiative effects must be carefully taken into account in the calculation of the total diabatic heating field. Less direct observations were available for extended clouds at great distances from the convective source but it was speculated (with the aid of extrapolation of the results pertaining to more vigorous disturbances) that radiative effects had become increasingly important. Such influences appear consistent with WMONEX observations of discrete regions of extended cloud precipitation.

Beyond further analysis of data, the development of models offers a potentially fruitful area of investigation. Using numerical techniques Brown (1979) tested the hypotheses that evaporative cooling of anvil rainfall explains the downdrafts observed below tropical systems. Brown's model was able to produce many of the features of such systems, although he neglected both radiative processes and cooling due to melting. However, we have noted that these two effects tend to cancel for the weakest of the Leary and Houze cases (case 2) which possesses rainfall most similar to that simulated by Brown (i.e., 0.5–1.0 mm h^{-1} compared to 0.3 mm h^{-1}). We have also noted that this need not be the case and that radiative effects may be of either major or minor importance. Consequently, a series of numerical studies is being undertaken using a model which includes a relatively sophisticated radiative model similar to that of Stephens and Webster (1979) thus catering to the radiation feedback processes discussed above. The primary aim is to develop a systematic estimate of the total diabatic heating field through the life cycles of convective systems and to obtain quantitative estimates of the broader question: the role of radiative processes in the tropical atmosphere over synoptic and climatological time scales.

Acknowledgments. The authors would like to thank Professors R. S. and J. S. Simpson, Professor R. A. Houze and Drs. C. M. R. Platt and E. J. Zipser for many helpful discussions during the course of this study. Thanks are also due to P. R. Brenton and P. A. Watterson for their help in analyzing data. This research was sponsored in part by the National Science Foundation under Grant ATM 78-14281A01.

REFERENCES

Albrecht, B., and S. K. Cox, 1975: The large-scale response of the tropical atmosphere to cloud modulated infrared heating. *J. Atmos. Sci.*, **32**, 16–24.

Brown, J. M., 1979: Mesoscale unsaturated downdrafts driven by rainfall evaporation. A numerical study. *J. Atmos. Sci.*, **36**, 313–338.

Cox, S. K., and K. T. Griffith, 1979: Estimates of radiative divergence during Phase III of the GARP Atlantic Tropical Experiment: Part II. Analysis of the Phase III results. *J. Atmos. Sci.*, **36**, 586–601.

Dopplick, T. G., 1972: Radiative heating of the global atmosphere. *J. Atmos. Sci.*, **29**, 1278–1294.

Greenfield, R. S., and T. N. Krishnamurti, 1979: The Winter Monsoon Experiment—report of December 1978 field phase. *Bull. Amer. Meteor. Soc.*, **60**, 439–445.

Heymsfield, A. J., 1972: Ice crystal terminal velocities. *J. Atmos. Sci.*, **29**, 1348–1357.

Houze, R. A., Jr., 1977: Structure and dynamics of a tropical squall-line system. *Mon. Wea. Rev.*, **105**, 1540–1567.

Leary, C. A., and R. A. Houze, Jr., 1979: Melting and evaporation of hydrometeors in precipitation from anvil clouds of deep tropical convection. *J. Atmos. Sci.*, **36**, 669–679.

Malkus, J. S., and H. Riehl, 1964: *Cloud Structure and Distribution over the Tropical Pacific Ocean*. University of California Press, Berkeley and Los Angeles, 229 pp.

Streten, N. A., 1973: Some characteristics of satellite observed bands of persistent cloudiness over the Southern Hemisphere. *Mon. Wea. Rev.*, **101**, 486–495.

Stephens, G. L., 1978: Radiative properties of extended water clouds, Part I. *J. Atmos. Sci.*, **35**, 2111–2122.

——, and P. J. Webster, 1979: Sensitivity of radiative forcing to variable cloud and moisture. *J. Atmos. Sci.*, **36**, 1542–1556.

——, and K. J. Wilson, 1980: The response of a deep cumulus convection model to changes in radiative heating. *J. Atmos. Sci.*, **37**, 421–434.

Webster, P. J., and D. Curtin, 1974: Interpretations of the EOLE Experiment II: Spatial variation of transient and stationary modes. *J. Atmos. Sci.*, **32**, 1848–1863.

Zipser, E. J., 1977: Mesoscale and convective scale downdrafts as distinct components of squall-line circulation. *Mon. Wea. Rev.*, **105**, 1568–1589.